Indian Journal of Chemistry
Vol. 56A, August 2017, pp. 832-837

Schiff base modified Pt electrode as sensor for detecting Al(III) and Pb(II)

Kangkana Deka & Diganta Kumar Das*
Department of Chemistry, Gauhati University, Guwahati 781 014, India
Email: diganta_chem@gauhati.ac.in

Received 5 April 2017; revised and accepted 27 July 2017

A platinum electrode with its surface modified with the condensation product of *p*-phenylenediamine and acetylferrocene (PPDA-AcFc) has been fabricated by cyclic voltammetry. The square wave voltammogram of the modified electrode, PPDA-AcFc/Pt, in aqueous medium gradually shifts by 0.440 V and 0.090 V in the positive direction on interaction with Al^{3+} and Pb^{2+} respectively. Electrochemical impedance spectroscopy shows the charge transfer resistance value of PPDA-AcFc/Pt electrode increases in the case of Al^{3+} while it decreases in the case of Pb^{2+}. The linear range of detection is 0-12 μ*M* and 0-6 μ*M* for Al^{3+} and Pb^{2+} respectively.

Keywords: Electrochemistry, Electrodes, Modified electrodes, Electrochemical impedance spectroscopy, Voltammetry, Aluminium, Lead

Although 8% of the earth's crust is Al^{3+} ion by mass, it does not play any biological role. While Al is not toxic, Al^{3+} ion is a neurotoxin and is reported to be linked with various neurodegenerative diseases including Alzheimer and Parkinson's disease. Al^{3+} ion causes oxidative damage of biological membranes[1-3], and is reported to cause osteoporosis, colic and rickets[4]. It also prevents Ca^{2+} uptake by plants leading to their retarded growth[5]. High concentration of Al^{3+} in human blood may cause impaired renal function[6,7]. Despite many drawbacks, use of Al cannot be avoided in modern life as it is essential for making electronic and electrical components of different gadgets, building materials, different packaging items, etc. Therefore, there is high probability of Al^{3+} contaminating the environment and hence affecting human health adversely. Thus, it is important to develop new analytical methods for the determination of Al^{3+} in water, foods, and biological fluids like blood and towards this, the designing a new sensor for detection of Al^{3+} is of high relevance.

Analytical techniques based on atomic absorption and emission spectroscopy[8,9], spectrophotometry[10], fluorescence[11], electroluminescence[12] are known for the detection of Al^{3+}. Due to the simplicity of operation, low cost, easy instrument maintenance, ready automation, etc., electrochemical techniques are gaining popularity for Al^{3+} detection[13]. Direct electrochemical determination of Al^{3+} by voltammetry is complicated because H_2 evolution occurs at potential near the Al^{3+} reduction potential which is –1.75 V versus Ag/AgCl as reference[14]. Modification of solid electrode has been an answer to avoid this complicacy, for example–carbon electrodes have been modified with dopamine[15], alizarin[16], 8-hydroxyquinoline[14,17], ionophore/polyvinylchloride[18,19], etc. for voltammetric detection of Al^{3+}. Molecular voltammetric probes for Al^{3+} have been reported based on 5-hydroxy-1-methyl-3H-benzo[ϕ]chromen-3-one[20]. Modified polyvinyl chloride (PVC) membrane with clinoptilolite nanoparticles/hexadecyltrimethyl ammonium bromide surfactant/Arsenazo III has been used for construction of Al^{3+}-selective electrode[21]. Al^{3+} selective electrode has also been prepared by coating the surface of a graphite rod by a membrane containing PVC as a plastic matrix, dibutylphthalate as plasticizer, 12C4 as an ionophore and oleic acid as an additive[22]. Gold electrode surface modified via covalent attachment of *p*-((8-hydroxyquinoline)azo) benzenethiol for selective Al^{3+} detection[23]. Electrodes modified by multi-walled carbon nanotubes and reduced graphene nanosheets are also known for Al^{3+} detection[24].

Due to its capability to mimic Ca^{2+}, Pb^{2+} occupies calcium binding sites on numerous calcium dependent proteins in cells, consequently resulting in impairment of physiological functions[25]. The sources of Pb^{2+} pollution to environment are printing industry, dyeing industry, lead glass manufacturing, etc.[26-29]. Methods well known for Pb^{2+} detection include atomic absorption spectrophotometry[30], inductively coupled plasma emission spectrometry[31] and fluorescence spectrometry[32,33]. Like Al^{3+}, electrochemical methods for Pb(II) detection also have gained popularity. Electrochemical sensor based on three-dimensional mesoporous graphene framework (MGF) has been developed for determination of Pb^{2+} in aqueous solution[34]. Graphene oxide textured with redox active Ru^{2+} bipyridine complex nanocomposite on Au electrode is reported for Pb^{2+} detection[35]. Ag NPs,

bismuth and Nafion modified carbon electrode is recently reported for detection of Pb^{2+} in aerosol[36]. Electrodeposition of reduced graphene oxide-gold nanoparticles nanocomposite film onto the surface of glassy carbon electrode followed by Nafion modification[37] was used for fabrication of an electrochemical sensor for trace amounts of Pb^{2+}. Nitrogen doped graphene/gold nanoparticle and Fe_2O_3@TiO_2 nanoparticle nanocomposite modified Au electrode[38] has been reported for Pb^{2+}. Porous honeycomb carbon with tunable size was synthesized and used as electrode material for Pb^{2+} detection[39]. Hollow silica microspheres containing amino groups has been synthesised and used as modifying agent for GC electrode for Pb^{2+} detection[40]. Copper based electrochemical sensor for Pb^{2+} by anodic stripping voltammetry has been reported[41]. Ion imprinted polymer using Pb^{2+} as a template was reported as Pb^{2+} ion selective voltammetric sensor[42]. Another voltammetric sensor for selective determination of Pb^{2+} is based on EDTA-immobilized graphene-like C nitride nanosheets[43]. Bismuth modified exfoliated graphite (EG) electrode for the co-detection of heavy metal ions –As^{3+}, Hg^{2+} and Pb^{2+}-in water samples using square wave anodic stripping voltammetry is reported[44]. In all the reported methods of electrode modification the modifying agents were synthesised chemically adopting relatively difficult synthetic methods.

Herein, we report a Pt electrode modified with the Schiff base obtained from p-phenylenediamine and acetylferrocene for detecting Al^{3+} and Pb^{2+} by cyclic voltammetry, square wave voltammetry and electrochemical impedance spectroscopy. Metal ions Li^+, Na^+, K^+, Mg^{2+}, Ni^{2+}, Cu^{2+}, Zn^{2+}, Cd^{2+}, Ce^{2+} and Hg^{2+} do not interfere.

Experimental

All the chemicals were purchased from Loba Chemie. The electronic spectra were recorded on a UV-1800 Shimadzu spectrophotometer. The FTIR spectra were recorded with KBr pellets (4000-400) cm^{-1} on a Perkin Elmer RXI FTIR system. High resolution mass (HRMS) spectra were recorded on an Agilent spectrometer using HPLC methanol as the solvent. CHI 600B electrochemical analyzer (USA) with a three electrode cell assembly was used for electrochemical studies. Electrochemical experiments were carried out under a blanket of nitrogen gas after passing the gas through the solution for 10 min. The working electrode was GC disc, reference electrode was Ag/AgCl (3 *M* NaCl) and $NaNO_3$ (0.1 *M*) was the supporting electrolyte. The square wave voltammetry (SWV) experiments were carried out at the square wave amplitude of 25 mV, frequency of 15 Hz and the potential height for base stair case wave front of 4 mV. The area of the Pt electrode was 0.025 cm^2.

For the synthesis of the sensor (PPDA-AcFc), solutions of 1 mmol (0.108 g) of *p*-phenylenediamine and 0.5 mmol (0.114 g) of acetylferrocene (AcFc) were prepared in dry CH_3OH (10 mL) separately. Both the solutions were mixed and the mixture was stirred for 24 h at room temperature. Blackish-brown shiny precipitate was obtained. The reaction mixture was allowed to stand till the solvent evaporated and dry product, PPDA- AcFc (I), was obtained. Yield: 96%, FTIR (cm^{-1}): 3432 and 3348 (ν_{NH2}); 1615 ($\nu_{C=N}$). HRMS m/z: 319.7606 (Calculated = 318.1933) (Supplementary data, Figs S1 and S2 respectively).

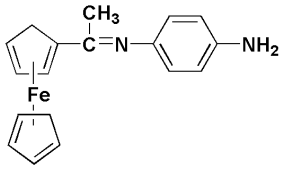

PPDA-AcFc

The Pt electrode was modified as follows: The Pt electrode was cleaned as reported[45] followed by sonication first in CH_3OH and then in water. The electrode was dried under a stream of N_2 gas. The cleaned electrode was placed in 0.1 *M* PPDA-AcFc in dry CH_3OH containing TBAP as the supporting electrolyte. Cyclic voltammetric runs carried out for 100 scan segments at scan rate 0.100 V s^{-1} show the increase in current indicates formation of film of PPDA-AcFc on Pt electrode surface (Fig. 1). The electrode was then gently washed with water and dried under a stream of N_2 gas and stored in refrigerator for further use. To further confirm the formation of the film of PPDA-AcFc, chronocoulogram of the modified electrode was recorded in water using 0.1 *M* $NaNO_3$ as supporting electrolyte (Fig. 1, Inset). A sharp decrease in charge versus time profile indicates adsorption of electroactive species onto the electrode surface, confirming formation of film of PPDA-AcFc on electrode surface. The modified electrode is designated as PPDA-AcFc/Pt henceforth in this paper. No redox peaks were observed when cyclic voltammogram was

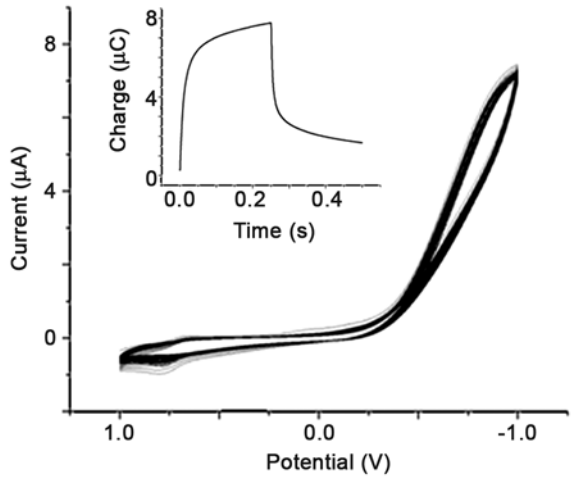

Fig. 1 — Cyclic voltammogram of Pt electrode in 0.1 *M* solution of PPDA-AcFc in dry CH_3OH containing TBAP as the supporting electrolyte for 100 scan at scan rate 0.1 V s^{-1}. Inset: Chronocoulogram of the modified electrode in water containing 0.1 *M* $NaNO_3$ as supporting electrolyte.

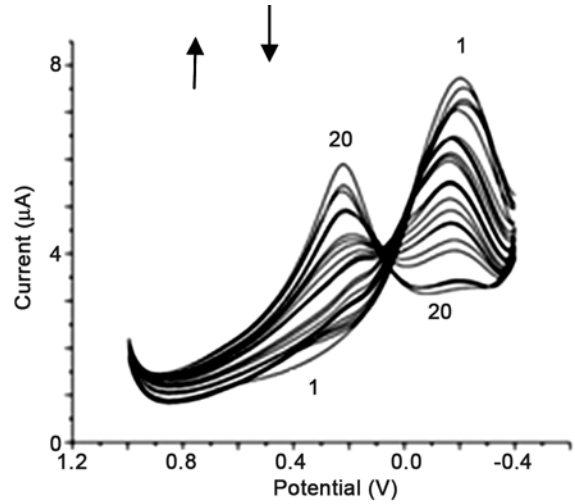

Fig. 2 — Square wave voltammograms of PPDA-AcFc/Pt electrode at different added concentration of Al^{3+} in water containing 0.1 *M* $NaNO_3$ as supporting electrolyte. (RE: Ag/AgCl). (1 and 20 indicates the first and twentieth scan respectively).

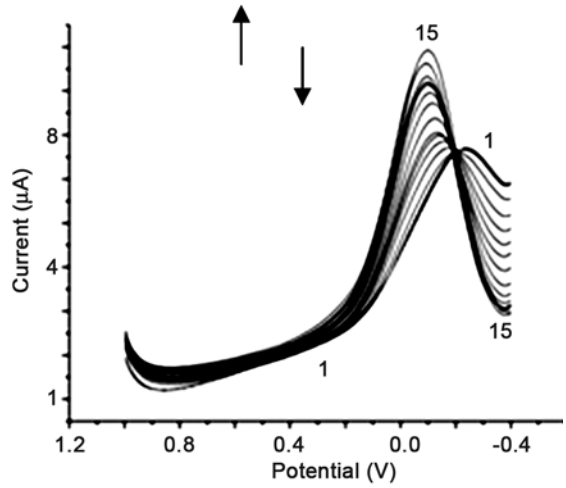

Fig. 3 — Square wave voltammograms of PPDA-AcFc/Pt electrode at different added concentration of Pb^{2+} in water containing 0.1 *M* $NaNO_3$ as supporting electrolyte. (RE: Ag/AgCl). (1 and 15 indicates the first and fifteenth scan respectively).

recorded in aqueous medium using the modified electrode. However, well defined redox peak at –0.210 V was observed on recording square wave voltammogram.

Results and discussion

Figure 2 shows the square wave voltammograms of PPDA-AcFc/Pt electrode at varying added concentration of Al^{3+} in the electrolytic medium. In the absence of Al^{3+}, a redox peak was observed at –0.210 V versus Ag/AgCl reference. This peak is due to $Fe^{2+/3+}$ redox couple of PPDA-AcFc. During electrochemical film deposition by CV no redox peaks were observed while square wave voltammetry could recognise one redox peak at –0.210 V. The nature of the film may be such that the CV is not sensitive enough to detect the redox process, but the more sensitive SWV could detect the redox peak.

Upon addition of Al^{3+}, the current of this peak decreases and a new peak starts appearing at +0.230 V versus Ag/AgCl reference. This process continues with increase in concentration of Al^{3+} up to 300 μ*M*. At this concentration, the current at –0.210 V is minimum and the current at +0.230 V is maximum. Further addition of Al^{3+} did not affect the current or peak position. Thus, addition of Al^{3+} may effect a significant 0.440 V positive shift in redox potential of the PPDA-AcFc/Pt electrode. Binding of Al^{3+} to PPDA-AcFc is probably through the lone pairs of electron on amine N. This binding of Al^{3+}, due to conjugation, would lead to a deficiency in electron density on Fe^{2+}. Thus oxidation of Fe^{2+} becomes difficult resulting in a positive shift in redox potential.

The effect of Pb^{2+} ion on the square wave voltammograms of AcFc/Pt electrode is shown in Fig. 3. The peak current at –2.10 V decreases with increasing Pb^{2+} concentration and a new peak appears at –0.120 V versus Ag/AgCl as reference electrode. The current at –0.120 V peak increases with Pb^{2+} ion concentration up to 300 μ*M* and remains constant thereafter. Thus the square wave voltammetric peak due to interaction between AcFc/Pt electrode and Pb^{2+} is 0.090 V more positive as compared to that of the AcFc/Pt electrode. Like Al^{3+}, Pb^{2+} also interacts with the

amine N of PPDA-AcFc leading to electron deficiency at Fe^{2+} and hence a positive shift. Since electron pulling capacity of Al^{3+} is higher than that of Pb^{2+} the electron deficiency at Fe^{2+} (of PPDA-AcFc) is more in the case of Al^{3+} than in Pb^{2+} and hence Al^{3+} could induce more positive shift in redox potential than Pb^{2+}.

Figure 4 shows the plot of redox peak currents of the PPDA-AcFc/Pt electrode as a function of

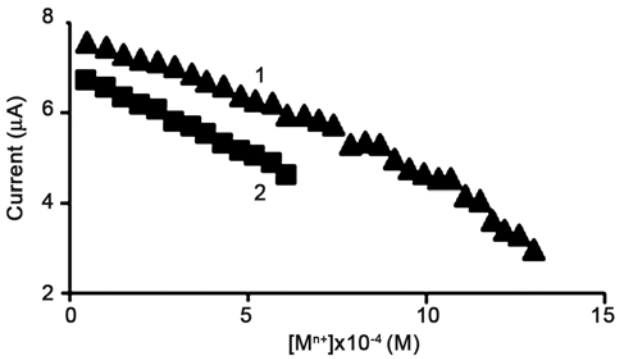

Fig. 4 — Plot of square wave voltammetric peak currents of PPDA-AcFc/Pt electrode at different added concentration of Al^{3+} (1, ▲) and Pb^{2+} (2, ■) in water containing 0.1 *M* $NaNO_3$ as supporting electrolyte. (RE: Ag/AgCl).

Al^{3+} concentration at redox potential –0.210 V. Good linearity between the peak currents and Al^{3+} concentration was observed with R^2 values 0.9654. Good linearity between the peak current and Pb^{2+} concentration was also observed with R^2 value 0.9732.

The EIS measurements of interaction between PPDA-AcFc/Pt electrode and Al^{3+} were made under optimised conditions as for square wave voltammetry at E_{DC} = 1.5V. Figure 5a shows the ESI Nyquist plot at different added concentration of Al^{3+} in the electrolytic medium. The R_{CT} was found to increase with increasing Al^{3+} concentration. Figure 5b shows the plot of ΔR_{CT} as a function of Al^{3+} concentration which was linear with R^2 value 0.9655.

The EIS measurements of interaction between AcFc/Pt electrode and Pb^{2+} were also made under optimised conditions as for square wave voltammetry at E_{DC} =1.5 V (Fig. 6a) at different added concentration of Pb^{2+}. Unlike in the case of Al^{3+}, the R_{CT} was found to decrease with increasing Pb^{2+} concentration. The plot of ΔR_{CT} as a function of Pb^{2+} concentration was linear with R^2 value 0.9672 (Fig. 6b).

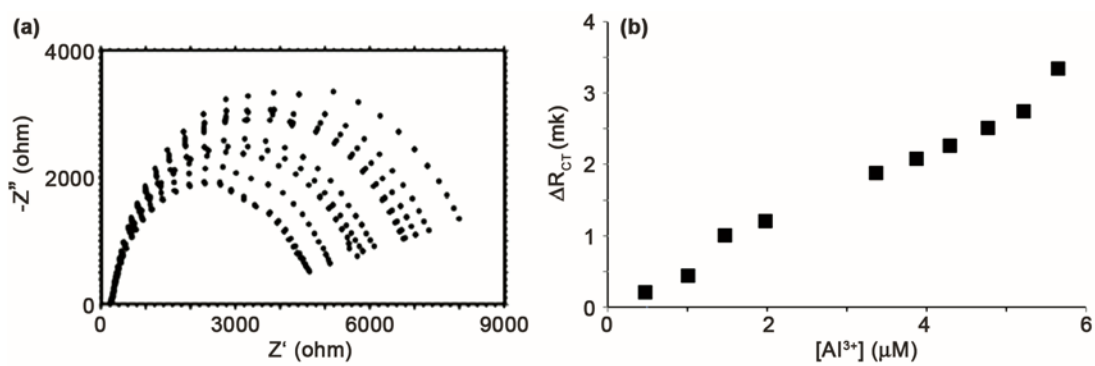

Fig. 5 — (a) Nyquist plot for PPDA-AcFc/Pt electrode at different added concentration of Al^{3+} in in water containing 0.1 *M* $NaNO_3$ as supporting electrolyte. (b) Plot of ΔR_{CT} versus Al^{3+} concentration.

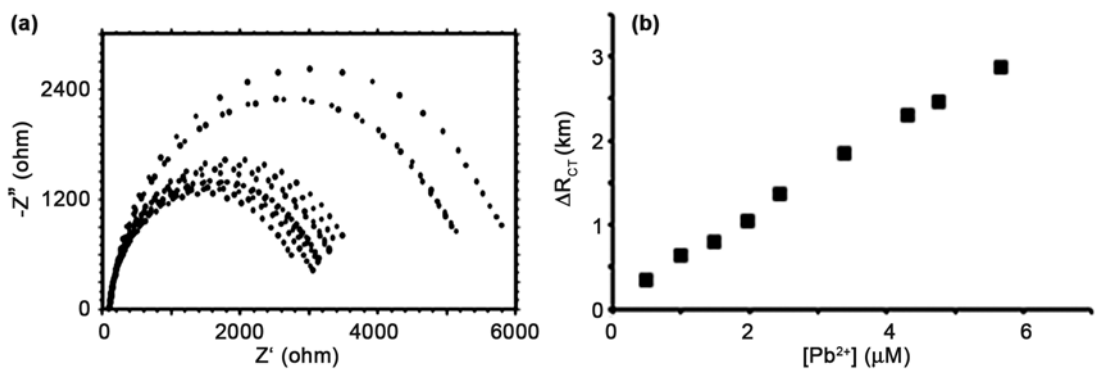

Fig. 6 — (a) Nyquist plot for PPDA-AcFc/Pt electrode at different added concentration of Pb^{2+} in in water containing 0.1 *M* $NaNO_3$ as supporting electrolyte. (b) Plot of ΔR_{CT} versus Pb^{2+} concentration.

Square wave voltammogram was recorded for PPDA-AcFc/Pt electrode in aqueous medium in presence of metal ions, i.e., Li^+, Na^+, Mg^{2+}, K^+, Ni^{2+}, Zn^{2+}, Cd^{2+}, Hg^{2+}, Ce^{2+} besides Al^{3+} and Pb^{2+}. No appreciable change in the square wave voltammogram was observed for these metal ions. The metal ions mentioned above other than Al^{3+} and Pb^{2+} do not bind to the sensor through $–NH_2$ lone pair electrons. Hence, they do not show any change in redox potential and current of the sensor. The bar diagram for the normalised current ($\Delta I/I_0$) obtained from square wave voltammogram of PPDA-AcFc/Pt electrode in aqueous medium in presence of 10^{-3} *M* interfering metal ions at +0.230 V and –0.120 V versus Ag/AgCl is shown in Fig. S1 (Supplementary data). Here ΔI is the difference in current in absence (I_0) and in presence of 10^{-3} *M* concentration of a particular metal ion. The interaction between PPDA-AcFc/Pt electrode is clearly seen and Al^{3+} is quite distinct over the other metal ions at +0.230 V. Similarly, the SWV confirms that PPDA-AcFc/Pt electrode can distinguish Pb^{2+} over the other metal ions at –0.120 V.

In conclusion, Pt electrode surface modified with condensation product of *p*-phenylenediamine and acetylferrocene (PPDA-AcFc) by cyclic voltammetry was found to shift its redox potential by 0.440 V in positive direction and by 0.090 V in negative direction respectively on interaction with Al^{3+} and Pb^{2+} respectively in aqueous medium. The normalised current was quite distinct for the modified electrode in presence of Al^{3+} and Pb^{2+} at applied potential +0.230 V and –0.120 V respectively. The charge transfer resistance value of PPDA-AcFc/Pt electrode, obtained from electrochemical impedance spectroscopy, shows increase in the case of Al^{3+} and decrease in the case of Pb^{2+}.

Supplementary data

Supplementary data associated with this article, viz., Fig. S1, is available in the electronic form at http://www.niscair.res.in/jinfo/ijca/IJCA_56A(08)832-837_SupplData.pdf.

Acknowledgement

Authors thank University Grants Commision, New Delhi and Department of Science & Technology, New Delhi, for financial support to the department through SAP and FIST respectively. IIT-Guwahati, North Guwahati, is thanked for HRMS.

References:

1 Budimir A, *Acta Pharm,* 62 (2011) 1.
2 Nayak P, *Environ Res,* 89 (2002) 101.
3 Zatta P, *Coord Chem Rev,* 228 (2002) 271.
4 Wang B, Xing W, Zhao Y & Deng X, *Environ Toxicol Pharmacol,* 29 (2010) 308.
5 Gensemer R W & Playle R C, *CR Environ*, 29 (1999) 315.
6 Medel A S, Cabezuelo A B S, Milacic R & Polak T B, *Coord Chem Rev,* 228 (2002) 373.
7 Hewitt C D, Wlnbome K, Margrey O, Nicholson J R P, Savory M G, Savory J & Wills M A, *Clin Chem,* 36 (1990) 1466.
8 Sang H, Liang P & Du D, *J Hazard Mater,* 154 (2008) 1127.
9 de Jesus D S, Gra M & Korn C, *Spectrochim Acta Part B,* 55 (2000) 389.
10 Abbasi S & Farmany A, *Food Chem,* 116 (2009) 1019.
11 Kumar J, Sarma M, Phukan P & Das D K, *Dalton Trans,* 44 (2015) 4576.
12 Muegge B D, Brooks M S & Richter M M, *Anal Chem,* 75 (2003) 1102.
13 Gupta V K, Jain A K & Maheshwari G, *Talanta* ,72 (2007) 1469.
14 Shervedani R K, Rezvaninia Z, Sabzyan H & Boeini H Z, *Anal Chim Acta,* 825 (2014) 34.
15 Zhang F, Yanga L, Bi S, Liu J, Liu F, Wang X, Yang X, Gan N, Yu T, Hu J, Li H & Yang T, *J Inorg Biochem*, 87 (2001) 105.
16 Akhtar P & Devereaux H A, *Anal Chim Acta,* 381 (1999) 49.
17 Cai Q & Khoo S B, *Anal Chim Acta,* 276 (1993) 99.
18 Arvand M & Asadollahzadeh S A, *Talanta,* 75 (2008) 1046.
19 Esmaelpourfarkhani M, Rounaghi G H & Arbab-Zavar M H, *J Brazil Chem Soc*, 26 (2015) 963.
20 Gupta V K, *Int J Electrochem Sci,* 10 (2015) 8770.
21 Mostafa M & Alireza N-Ejhieh, *J Colloid Interface Sci,* 494 (2017) 317.
22 Masoomeh E, Gholam H R, Mohammad H A-Zavar, *J Brazil Chem Soc,* 26 (2015) 963.
23 Karimi S R, Z Rezvaninia, Hassan S & Hassan Z B, *Anal Chim Acta,* 825 (2014) 34.
24 Tang Y-Zheng, Chen X, Yang Xu-Jie, Shen Ren-Fang, Yang X-Di & Xu C-Zheng, *IEEE Sensors,* J 13 (2013) 3270.
25 Lewis J A & Cohen S M Addressing, *Inorg Chem,* 43 (2004) 6534.
26 Deng Y, Gao Z, Liu B, Hu X, Wei Z & Sun C, *Chem Eng J,* 223 (2013) 91.
27 Cui L, Xu W, Guo X, Zhang Y, Wei Q & Du B, *J Mol Liq,* 197 (2014) 40.
28 Alaparthi M & Sykes A G, *J Incl Phenom Macrocycl Chem,* 83 (2015) 149.
29 Behbahani M, Bide Y, Salarian M, Niknezhad M, Bagheri S, Bagheri A & Nabid M R, *Food Chem*, 158 (2014) 14.
30 Jurado J M, Martín M J, Pablos F, Moreda-Pineiro A & Bermejo-Barrera P *Food Chem,* 101 (2007) 1296.
31 Ho T Y, Chien C T, Wang B N & Siriraks A, *Talanta,* 82 (2010) 1478.
32 Guzman-Mar J L, Hinojosa-Reyes L, Serra A M, Hernández-Ramírez A, Cerdà V, *Anal Chim Acta,* 708 (2011) 11.
33 Das D K, Goswami P & Sarma S, *J Fluoresc,* 23 (2013) 503.
34 Xiao L, Wang B, Ji L, Wang F, Yuan Q, Hu G, Dong A & Gan W, *Electrochim Acta,* 222 (2016) 1371.
35 Gumpua M B, Veerapandian M, Krishnand U M & Rayappan J B B, *Talanta*, 162 (2017) 574.
36 Mettakoonpitak J, Mehaffy J, Volckens J & Henry C S, *Electroanal,* 28 (2016) 1.

37 Zhao G, Wang H, Liu G, Wang Z & Cheng J, *Ionics*, 23 (2017) 767.
38 Liu F-mei, Zhang Y, Yin W, Hou-jun, Huo D-qun, He B, Qian L-lin & H-bao F, *Sensors Actuators B*, 242 (2016) 889.
39 Xu R, Xiao L, Luo L, Jia H, Wang C & Wang F, *J Electrochem Soc,* 164 (2017) B382.
40 Hao He-Qun, Xie Lei, Jin Jun-Cheng, Wu Ju, Xie Cheng-Gen & Fu Xu-Cheng, *J Electrochem Soc,* 163 (2016) H1081.
41 Kang W, Pei X, Rusinek C A, Bange A, Haynes E N, Heineman W R & P Ian, *Anal Chem,* 89 (2017) 3345.
42 Hu S, Xiong X, Huang S & Lai X, *Anal Sci* 32 (2016) 975.
43 Teng Z, Lv H, Wang L, Liu L, Wang C & Wang G, *Electrochim Acta,* 212 (2016) 722.
44 Mafa P J, Idris A O, Mabuba N & Arotiba O A, *Talanta,* 153 (2016) 99.
45 Rajbangshi J, Das D K & Mazumder S, *Electrochim Acta,* 55 (2010) 4174.